Study the effect of wear rate on impingement failure of an acetabular liner surface based on finite element analysis

Eko Saputra*, Iwan Budiwan Anwar and Emile van der Heide

Laboratory for Surface Technology and Tribology,
Faculty of Engineering Technology, University of Twente
Drienerloolaan 5, Postbox 217, 7500 AE, Enschede, The Netherlands.
Email: ekosaputro984@gmail.com
Email: iwanbudiwan@yahoo.com
Email: E.vanderHeide@utwente.nl
*Corresponding author

Rifky Ismail and J Jamari

Laboratory for Engineering Design and Tribology,
Department of Mechanical Engineering, Diponegoro University,
Jl. Prof. Soedharto SH, Tembalang, Semarang 50275, Indonesia.
Email: r_ismail@undip.ac.id
Email: j.jamari@gmail.com

Abstract: In this study, correlation of wear inside of an acetabular liner surface (ALS) and damage on an acetabular liner rim (ALR) due to impingement effect are investigated. The analysis included evaluation of the macrostructure of the damage based on visual investigation and computer simulation analysis. A commercial finite element method ABAQUS software package is used to simulate local impingement on the ALR due to wear depth variations (wear rates) inside the ALS. Here, the wear depth is based on the data of wear experiment from literature. The von Mises stress and contact deformation on the ALR at impingement is presented. In addition, the initial impingement angle is also presented to show the correlation between the wear inside of the ALS and the angle of impingement occurrence. The results show that the existence of wear inside of the ALS can increase the damage of the ALR due to impingement effect.

Keywords: acetabular liner; finite element analysis; impingement; wear rate.

Reference to this paper should be made as follows: Saputra, E., Anwar, I.B, Ismail, R., Jamari, J., and van der Heide, E. (2015) ‘Study the effect of wear rate on impingement failure of an acetabular liner surface based on finite element analysis’, Int. J. Materials and Product Technology, Vol. xx, No. 1/2/3/4, pp.xxx–xxx.

Biographical notes: Eko Saputra is a PhD candidate at the University of Twente, the Netherlands. He received his MSc at the University of Diponegoro in 2012. In 2013, he was awarded by Taiho Kogyo Research Foundation

(TTRF) Award for Young Tribologist. His areas of scientific interests are in finite element analysis (FEA), product design, and tribology. He has published papers in several international proceedings and journals.

Iwan Budiwan Anwar is an orthopedist at the dr. Soeharso national orthopedic hospital, Solo, Indonesia. He is also a PhD candidate in BioMechanical Engineering at Surface Technology and Tribology, University of Twente. His areas of scientific interests are hip joint replacement and design of implants. He has published papers in several international proceedings and journals.

Emile van der Heide has been working in the Laboratory for Surface Technology and Tribology, Faculty of Engineering Technology, University of Twente as professor of chair of skin Tribology since 2009. In 2002, he received his Doctor in Mechanical Engineering from University of Twente, The Netherlands. His areas of scientific interests are bio-tribology and metal forming. He has published many papers in several major tribology journals.

Rifky Ismail is a lecturer at the University of Diponegoro, Semarang, Indonesia. In 2013, he received his Doctor in Mechanical Engineering from the University of Twente, The Netherlands. His areas of scientific interests are engineering design and wear. He has published papers in several international proceedings and journals.

J Jamari is a lecturer at the University of Diponegoro, Semarang Indonesia. He had been working in the Surface Technology and Tribology, the University of Twente, the Netherlands. He received his Bachelor and Master from Institute of Technology Bandung, Indonesia. He received his Doctor in Mechanical Engineering from the University of Twente, The Netherlands in 2006. His areas of scientific interests are engineering design and tribology. He has published papers in several international proceedings and journals.

1 Introduction

Dislocation is one of the main problems of total hip arthroplasty patients during their daily activities (Sikes et al., 2008). Two types of dislocation can be distinguished to be an early dislocation and late dislocation (Cuckler, 2011). In general, the early and late dislocations are mostly related to impingement between the neck stem against the acetabular liner rim and wear inside of the acetabular liner surface, respectively (Cuckler, 2011; Hummel et al., 2009). For the early dislocation, impingement is induced by the limitation of range of motion (RoM) of the total hip arthroplasty patient's artificial hip joint. The excessive human activities can induce a higher range of motion and cause impingement. The activities of the total hip arthroplasty patients as well as its implication for the range of motion and impingement have been reported. According to this, Sugano et al. (2012) presented the measurement of the RoM for Western and Japanese style activities. Recently, Saputra et al. (2013-2014) found that impingement and dislocation are predicted to be occurred in picking up activities for the combination of inclination and anteversion in the acetabular liner cup of 45°and 15°, respectively.

Additionally, after total hip revision is done, it is found that the wear in the late dislocation can increase the impingement as a part of early dislocation. It is indicated by the wear phenomenon inside the acetabular liner surface that is sometimes followed by damage on the acetabular liner rim. This can be examined from visual inspection of an orthopedic specialist. There is not many literature discuss the contribution of wear inside the acetabular liner surface to the damage on the acetabular liner rim. By finite element simulation, Scifert et al. (1998) modified the acetabular linear design (chamfer bevel angle, lip breadth, head center inset) to investigate the peak intrinsic moment developed to resist dislocation, and the ranges of motion before neck on lip impingement and before frank dislocation. The result showed that in every millimeter of the increased head center inset, the peak moment resisting dislocation increases 5.8%. Tanino et al. (2007) found that the acetabular liner articular geometry, which is the depth of the articular surface, is relative to the acetabular liner rim. It is also related to the prevalence of dislocation based on clinical data. This phenomenon is possible because the wear inside of the acetabular liner is shifted to the center point of the femoral head; consequently it will increase the head center inset. Based on the aforementioned literature, it can be noticed that the wear of the acetabular liner surface affecting the impingement cannot be avoided. Hence, the knowledge of the relation between the wear inside of the acetabular liner surface and the impingement on the acetabular liner rim is important. On the other hand, description of the impingement process due to existence wear inside of the acetabular liner surface and contribution of wear to the damage rate on the acetabular liner are still unclear.

In the work of Scifert et al. (1998), the increased of peak moment resisting was not due to wear inside of the acetabular liner surface but it was due to the modification of the head inset center. Therefore, there was no correlation between the wear and the damage on the acetabular liner rim. Similar result was also found by Tanino et al. (2007). There is no explanation how the contributions of wear at the inside of the acetabular liner surface to the damage on the acetabular liner rim. Theoretically, the wear rate of the acetabular liner surface can be predicted. Hence, the impingement due to wear can also be predicted by considering the wear rate. The objective of the present study was to investigate the effect of wear rate inside of the acetabular liner surface to impingement on the acetabular liner rim. In this study, the impingement process was simulated using commercial finite element analysis software package ABAQUS by varying the wear depth inside of the acetabular liner surface, based on specific wear rates obtained from literature.

2 Method

2.1 Hypothesis of the case

The acetabular liner is placed between the acetabular cup (shell or cup) and the femoral head (ball) in a unipolar of artificial hip joint. The artificial hip joint and location of acetabular liner can be seen in Figure 1(a). In general, the acetabular cup and femoral head are made from metal; while the acetabular liner is made from an ultra-high molecular weight polyethylene (UHMWPE) material.

Based on the visual investigation of the acetabular liner revision, which is obtained from orthopedic hospital Soeharso in Indonesia, two damages on the acetabular liner were found, see Figure 1(b). First one is on the acetabular liner rim and the second one is inside of the acetabular liner surface. First damage is predicted due to the repeated impingement effect between neck stem and acetabular liner rim (Jamari et al., 2014). Second damage is the wear, where it is caused by friction between the femoral head and Acetabular liner surfaces.

This case is interesting since the existence of high damage on the acetabular liner rim together with the presence of wear inside of the acetabular liner surface. These phenomena indicate that both wear inside the acetabular liner surface and impingement effects on the acetabular liner rim have correlation. Hypotheses of this damage are caused the center point of the femoral head shift from the condition before wear towards the condition after wear, it will cause the free range of motion remittent, and therefore it will cause the impingement occurrence faster than normal condition without wear. The essential is the existence of wear inside the acetabular liner surface can affect to damage on the acetabular liner rim. Yet, the increase wear depth will increase the impingement effect.

Figure 1 (a) Location of / at the acetabular liner of artificial hip joint and (b) the acetabular liner with damage in acetabular liner rim and wear inside of the acetabular liner surface

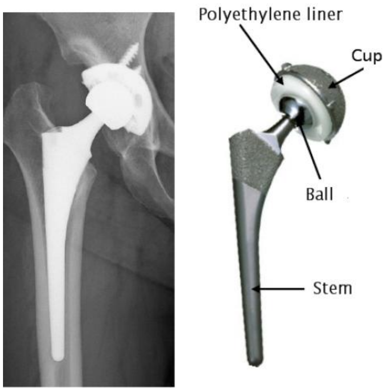

(a)

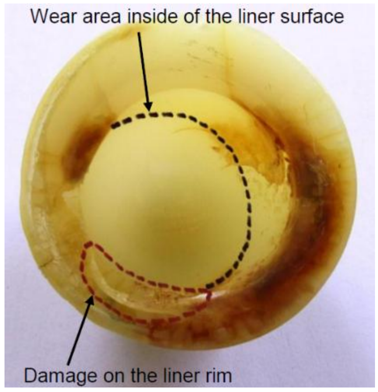

(b)

2.2 Finite element analysis

The simulation in this paper is divided into two steps, i.e. the static contact of femoral head against the acetabular liner and the rotation of femoral head against the acetabular liner until impingement. To reach it, creating the geometry model, defining the material properties of femoral head and acetabular liner, creating the simulation procedure and obtaining the result data need to be performed.

2.2.1 Geometry model

In simulation process, a three dimensional model of femoral head and acetabular liner are created using CAD software. The acetabular cup is not involved in this simulation because it can be represented as fixed constraint on the outer surface of acetabular liner. Dimensions of femoral head and acetabular liner are adopted in the femoral head and acetabular liner of Dowson experiment, see Table 1. Model of femoral head and acetabular liner with dimensions can be seen in Figure 2. Variable of RH (radius of the femoral head) and RL (radius of liner) are appropriated with diameters in Table 1. The diameter of neck stem is 14.2 mm. The acetabular liner has inset 2 mm and chamfer angle 45^{O}.

Table 1 Dimension of acetabular liner and femoral head

Components	Diameter (mm)
Acetabular liner 1	32.5458

Acetabular liner 2	32.5340
Femoral head 1	31.9800
Femoral head 2	31.9400
Neck stem	14.2

Figure 2 Dimension of (a) femoral head with neck stem and (b) acetabular liner with chamfer

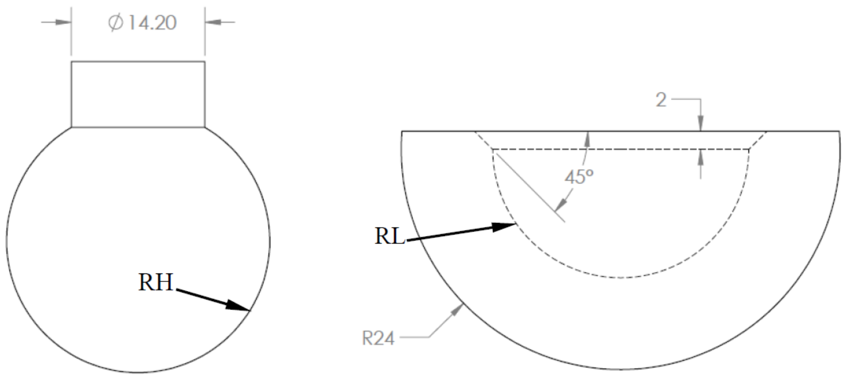

(a) (b)

Figure 3 (a) The illustration of artificial wear inside of acetabular liner and (b) the wear depth of acetabular for two acetabular liners as a function of loading cycles under normal walking condition (Dowson et al., 1993)

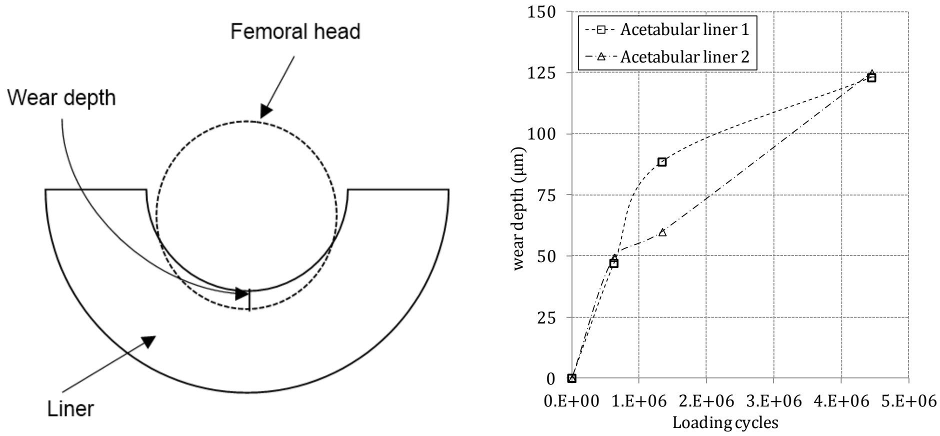

(a) (b)

An artificial wear inside of the acetabular liner surface to provide the simulation requirement was created. With simple techniques, the artificial wear can be created using cut revolve feature in CAD software. The shape of artificial wear is based on the wear depth and the diameter of femoral head in Table 1. The shape of artificial wear is created with the assumption that the wear shape is appropriate with the radius of the femoral head, see Figure 3(a). The implementation of wear depth in here is using the wear depth data from Dowson's experiment (Dowson et al., 1993). Dowson et al. (1993) investigated the wear inside two acetabular liner surfaces using hip simulator apparatus. Where, the dimensions of each femoral head and acetabular liner follow Table 1. Dowson et al. (1993) presented the progress of wear depth as a function of loading cycle under normal walking conditions, see Figure 3(b).

In this work, wear is modelled as a geometrical cut inside of the acetabular liner surface without consider lubrication regime. Contact condition in this simulation is assumed as a dry contact. Furthermore, this simulation does not focus on the wear prediction but it is only to investigate the correlation between the wear inside of the acetabular liner surface with the impingement progress on the acetabular liner rim.

2.2.2 Material properties

In general, the femoral head and acetabular liner are made from metal or ceramic and an ultra-high molecular weight polyethylene (UHMWPE) material respectively. To simplify, the femoral head is assumed as rigid body because the femoral head is harder, whereas the acetabular liner is assumed as deformable. Material model of UHMWPE model is assumed as an isotropic strain hardening elastic-plastic material model, where it is developed by stress-strain curve data from tensile test. The data of true stress-strain curve from tensile test of UHMWPE material is obtained from Kurtz et al. (1998), see Figure 4.

Figure 4 True stress vs true strain of UHMWPE material (Kurtz et al., 1998)

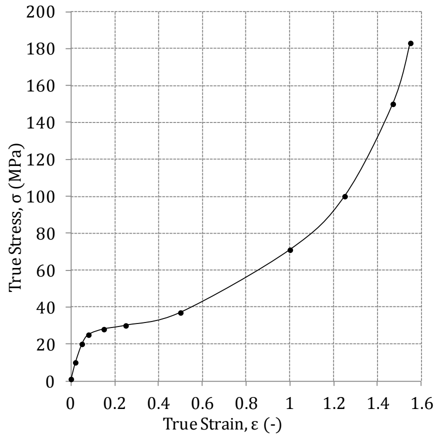

To finite element simulation requirement, the stress-strain curve is discretized where it is similar to that used by McNie et al. (1998) and Faulkner and Arnell (2000). This model assumed an elastic modulus of 850 MPa (Dowson et al., 1993) and an initial yield stress of 20 MPa.

2.2.3 Simulation procedure

The finite element simulation in this study is performed using Abaqus software version 6.12. In the real condition, the assembly of femoral head and acetabular liner is arranged based on inclination and anteversion angles. To simplify this, here, the simulation of the femoral head against acetabular liner is arranged in an ordered level, see Figure 5. The simulation consists of two steps, i.e. static contact and rotation steps. The static contact step is the femoral head pressing the acetabular liner with applied load F = 3000 N, where the applied load is placed in the center point of femoral head. This applied load adopts the vertical load from Dowson experiment. In the rotation step, the femoral head is rotated in z-axis rotation with angle $\theta = 1.1$ radian (for Abaqus input) or $\theta = 63.03^{o}$. The magnitude of this angle is a user-defined, or it is set towards impingement occurrence between the neck stem surfaces with the acetabular liner rim. In the static contact step, the center point of the femoral head is constrained in all axis directions except in y-direction. In the rotation step, the y and z axes rotation is free constraint. The outer surface of acetabular liner is fixed. All of these settings can be seen in Figure 5.

Figure 5 The 3D model of femoral head against acetabular liner include the applied load, constrained, mesh and rotation direction

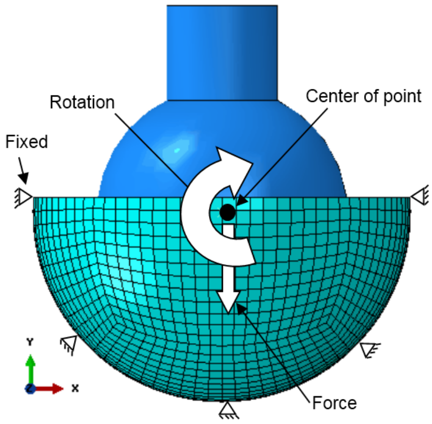

The element type that used in the acetabular liner is an 8-node linear brick, reduced integration, as well as hourglass control (C3D8R), where the numbers of elements are around 6,500 elements. This element type is recommended for modeling of continuum solids. The continuum elements can be used for linear analysis and complex non-linear analyses involving contact, plasticity and large deformations. It also usually provides a solution of equivalent accuracy at less cost (Abaqus 6.12 doc., 2012). The femoral head cannot be meshed due to the rigid body. The numbers of simulations are eight simulations with wear depth variation based on wear depth for two acetabular liners and femoral head, see figure 3 (b).

2.2.4 Post-processing

After finishing the simulation process, the next step is obtaining data from the simulation results. Several procedures to obtain data of the results are needed to be created. There are three proposed procedures, i.e. collecting data of von Mises stress at impingement, collecting data of impingement angle and collecting data of deformation on the acetabular liner rim due to impingement contact.

2.2.4.1 The von Mises stress at impingement

The data of von Mises maximum stress at impingement is needed to understand the relation of von Mises stress on the acetabular liner rim at impingement due to wear inside the acetabular liner surface. In ABAQUS software, the von Mises stress can be read in the field output S-Mises (von Mises stress). The von Mises stress is obtained when the rotation of femoral head reaches angle $\theta = 1.06$ radian or $\theta = 60.73^{o}$, where the angle θ is obtained from an initial impingement angle, see illustration in Figure 6. The initial impingement angle will be explained in the next chapter.

Figure 6 The illustration of obtaining von Mises stress at impingement

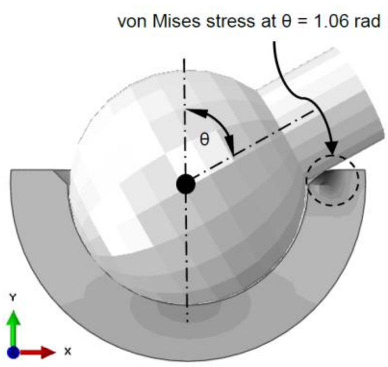

2.2.4.2 Initial impingement angles

The data of initial impingement are needed to understand the relation of impingement angle progress due to wear inside the acetabular liner surface. In Abaqus software, the angle of rotation in z-axis can be read in the field output UR3 (rotational displacement). Availability of UR data depends on step frame that required by Abaqus to solve the simulation of case. In this case, the UR data are appropriate with step frame. In other words, the more step frame is resulted in the more accurate angle. There are two types of step frame, i.e. automatic and fixed type. In the automatic one, the step frame that resulted is irregular, whereas the fixed one, the step frame that resulted is regularly appropriate with user-defined. To obtain the accurate data of initial impingement angle, the smooth step frame is required. As the consequence, it will take long time and require high convergence. Therefore, another method to obtain the initial impingement angle is required.

Figure 7 The procedure to obtain the initial impingement angle

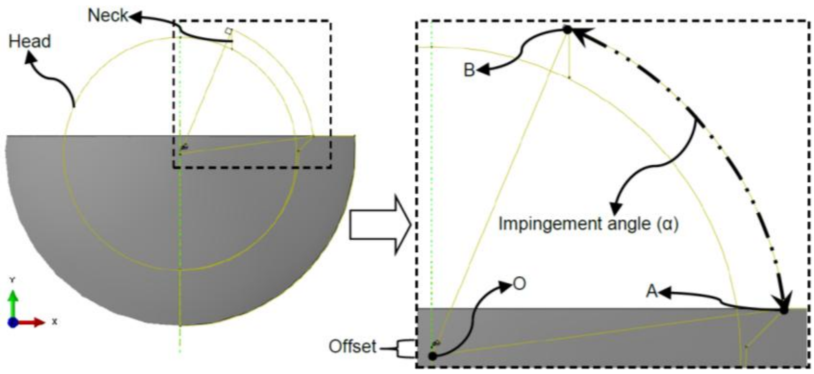

In this paper, the method that is used to take the initial impingement angle is sketching method. The initial step is conducted by sketching the acetabular liner with chamfer and femoral head with neck stem. The main concern of this method is the placement distance of the center point position of the femoral head to the center point of the acetabular liner. In this paper, it is called as offset of center points. The magnitude of this offset is the addition of the difference of a radius between the femoral head and the acetabular liner; wear depth and deformation contact due to static contact. The value of contact deformation is obtained from the result of simulation, where the value of this contact deformation depends on the applied load. If only consider the wear effect of the initial impingement angle, the contact deformation can be neglected. In fact, the contact deformation is always exist due to the human body weight. Therefore, in this paper, the initial impingement angle with and without the contact deformation will be presented as a comparison.

After the applied offset, the new center point of the femoral head is found. Further, the circle with the new center point as circle center point ‘O’ is created. The circle radius is the length of the center point ‘O’ to point chamfer ‘A’. The new circle will cut the neckline and resulted in cut point B. By connecting the point of O, A and B, the angle of AOB is formed. This angle is called as the initial impingement angle.

2.2.4.2 Contact deformation on the acetabular liner rim at impingement

In addition to the von Mises stress on the acetabular liner rim and the initial impingement angle of impingement contact due to wear inside the acetabular liner surface, the progress data of contact deformation on the impingement contact point are needed. The data of contact deformation are obtained on the acetabular liner rim, see Figure 8. The contact deformation is taken along with the impingement process until the rotation angle reaches θ = 1.1 radian. The contact deformation that is investigated on the acetabular liner rim is a deformation in y-axis direction. In ABAQUS software, the displacement in y-axis can be read in the field output U2 (y-displacement).

Figure 8 The procedure to obtain the data of contact deformation

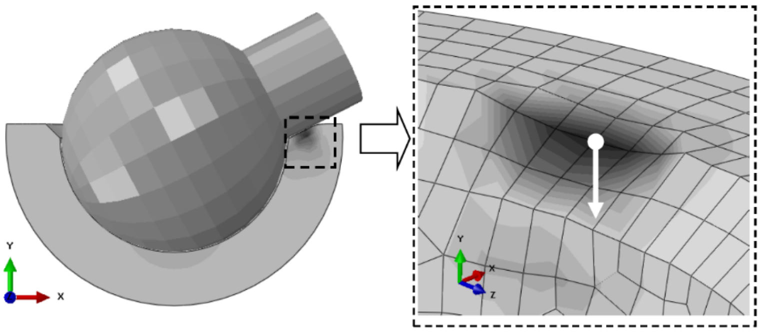

3 Results and discussion

In the previous work (Saputra et al., 2013), the similar impingement simulation that consists of the load and rotation step had been performed, then it is used as a validation process. The different is only from the position of assembly between the head and the liner, where in this work does not applying the inclination and anteversion angles.

3.1 The maximum of von Mises stresses on the acetabular liner rim

Figure 9 shows the progress of von Mises maximum stress on the acetabular liner rim at impingement or at the rotation of femoral head reach angle θ = 1.06 radian or θ = 60.73^{o}. Based on Figure 9, the von Mises maximum stress increases along with the increasing wears depth. Logically, when the center point of femoral head shifts due to existence of wear inside of the acetabular liner surface, it will cause the impingement to occur faster.

Figure 9 The von Mises maximum stress of impingement contact as a function of wear depth inside of the acetabular liner surface

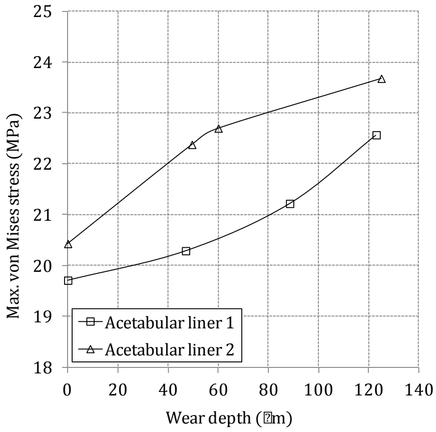

Figure 10 The von Mises maximum stress on the acetabular liner rim along with impingement for (a) without wear, (b) with wear no. 1, (c) with wear no. 2 and (d) with wear no. 3

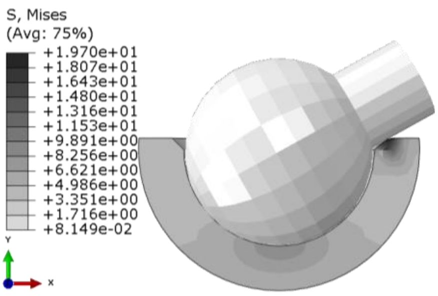

(a)

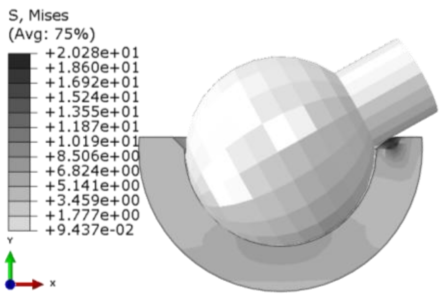

(b)

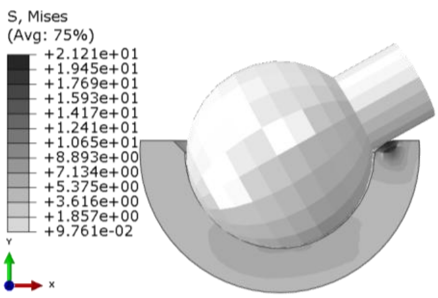

(c)

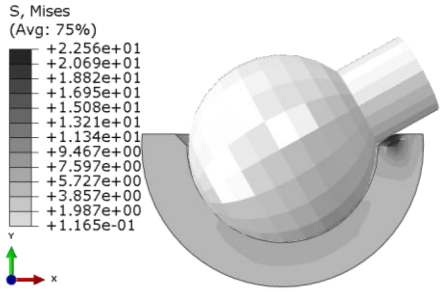

(d)

With the same angle of rotation for all wear variations, it will cause the stress in the impingement contact to increase. It is proven by the increasing of von Mises stress along with the wear variation. To show the position of von Mises maximum stress in the acetabular liner rim for each wear variation, as representation, the von Mises maximum stress on the acetabular liner rim number 1 is presented, see Figure 10.

3.2 The initial impingement angles

Figure 11 shows the progress of the initial impingement angle of the femoral head till it reaches the initial impingement caused by wear depth in acetabular liner surface. There are two results in Figure 11, i.e. the initial impingement angle with and without considering of contact deformation. The contact deformation in here is caused by the static contact process. Based on Figure 11, the initial impingement angle with contact deformation has faster impingement than the initial impingement angle without contact deformation. It is caused by the larger offset had by the former rather than the later. In fact, the contact deformation in this case cannot be neglected, so the offset with contact deformation as data input in the sketching method should be included.

Based on Figure 11, both of the initial impingement angles with or without considering the contact deformation show that the progress of initial impingement angle decrease along with the progress of wear depth. It can be explained that the existence of wear inside the acetabular liner surface has contributed to the initial impingement angle. The increasing wear depth inside of the acetabular liner surface can accelerate the impingement occurrence on the acetabular liner rim.

Figure 11 The impingement angle occurrence on the acetabular liner rim as a function of wear depth

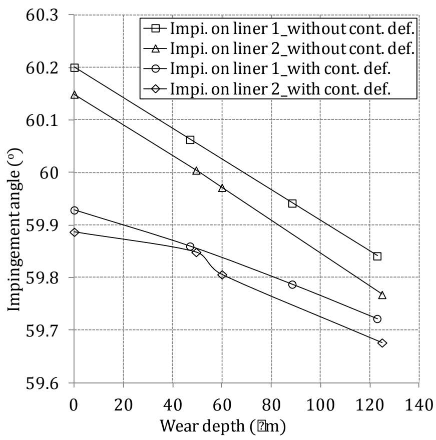

3.3 The contact deformation on the acetabular liner rim

The impingement contact between the neck stem surface and acetabular liner rim has an effect. The larger effect of this impingement on the acetabular liner rim is deformation. Figures 12 (a) and 12 (b) show the progress of contact deformation on the acetabular liner rim along with impingement process till angle θ = 1.1 radian for two acetabular liner. The taking of deformation starts at an impingement angle θ = 60° at until θ = 63°. Based on the previous section, the von Mises maximum stress for both models of acetabular liner 1 and 2 exceed the yield stress, therefore the contact deformation in this case is categorized as elastic-plastic deformation.

Based on Figure 12, the progress of contact deformation in two acetabular liner rims is increasing along with impingement process. As mentioned before, it can be similarly explained as the von Mises stress explanation. Logically, when the center point of femoral head shifts due to the existence of wear inside of the acetabular liner surface, it will cause the impingement to occur faster. With the same angle of rotation for all wear variations, it will cause the deformation on the acetabular liner rim due to impingement contact to increase. It is proven by the increasing of deformation on the acetabular liner rim along the wear variation.

Figure 12 Deformation of the acetabular liner rim at impingement reach angle θ=1.1 radian, (a) on the acetabular liner 1 and (b) on the acetabular liner 2

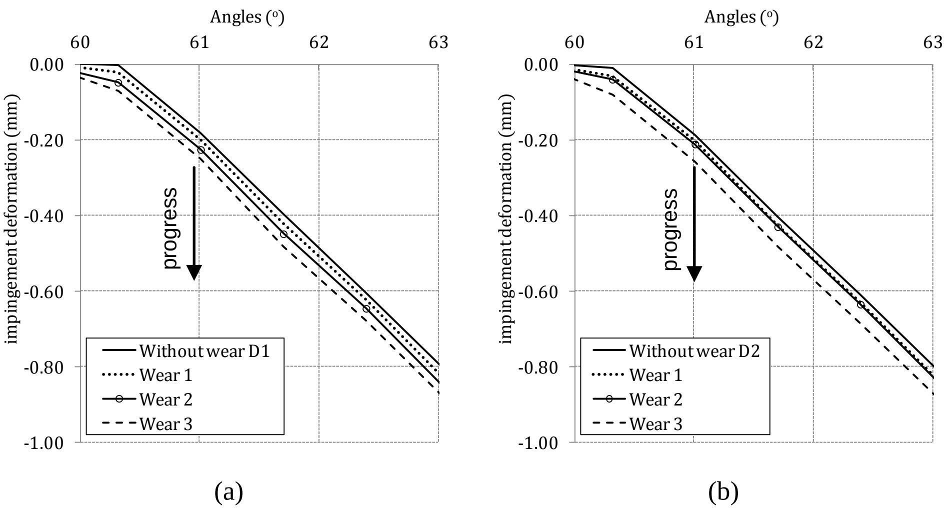

Based on the phenomena that are explained in these results, it can be understood that the damage rate on the acetabular liner rim is proportional to the increase of wear depth inside of the acetabular liner surface. This research has successfully confirmed the previous research (Tanino et al., 2007; Scifert et al., 1998). Besides, the repeated impingement due to human daily activities will give contribution to the damage rate on the acetabular liner rim; it is similar to previous studies (Jamari et al., 2014). In the present study, a fatigue and cyclic loading are not investigated. This research only investigates the correlation between the wear inside of the liner surface and the impingement on the liner rim. Yet, the damage on the liner rim can also be studied as a result of the cyclic loading or fatigue effect.

4 Conclusion

Study the relation of wear depth progress inside of the acetabular liner surface to impingement progress on the acetabular liner rim has been performed. To investigate this relation, the impingement simulation of femoral head against acetabular liner with the artificial wear is performed using Abaqus software. The artificial wear is created using cut revolve feature in CAD software based on the wear depth and the radius of the femoral head. The impingement simulations are divided into two steps, i.e. static contact and rotation simulation of femoral head against the acetabular liner.

Based on the results, it can be concluded that the existence of wear inside of the acetabular liner surface can increase the damage to the acetabular liner rim. It is caused by the shift of the center point of the femoral head towards inside of acetabular liner and it causes the range of movement to decrease. The decreasing of free range of motion will accelerate the impingement process. It is proven based on the measurement of impingement angle, where the impingement angle increases along the wear depth progress inside of the acetabular liner surface. Additionally, it can be also proven with the progress of maximum von Mises stress at impingement and the progress of contact deformation on the acetabular liner rim during impingement.

The progress of maximum von Mises stress on the acetabular liner rim at the impingement is increased along with the progress of wear inside the acetabular liner surface. Yet, the contact deformation on the impingement between neck stem surface and the acetabular liner rim is increased along with impingement process. All results of this research confirm that the wear rate inside the acetabular liner surface will increase the damage on the acetabular liner rim due to the impingement contact.

Acknowledgements

The authors would like to thank the Malaysian International Tribology Conference 2015 (MITC2015). The work was originally accepted for and presented at MITC2015.

References

ABAQUS (2012) `ABAQUS Documentation', Dassault Systèmes, Providence, RI, USA.

Cuckler, J.M. (2011) 'The dislocated total hip: the dreaded 3 AM phone call', *Semin. Arthro.*, Vol. 22, pp. 98-99.

Dowson, D., Jobbins, B. and Seyed-Harraf A. (1993) 'An evaluation of the penetration of ceramic femoral heads into polythene acetabular cups', *Wear*, Vol. 162-164, pp. 880-889.

Faulkner, A. and Arnell, R.D. (2000) 'The development of a finite element model to simulate the sliding interaction between two, three-dimensional, elastoplastic, hemisperichal asperities', *Wear*, Vol. 242, No. 242, pp. 114-122.

Hummel, M.T., Malkani, A.L., Yakkanti, M.R. and Baker D.L. (2009) 'Decreased dislocation after revision total hip arthroplasty using larger femoral head size and posterior capsular repair', *J. Arthrop.*, Vol. 24, No. 6, pp. 73-76.

Jamari, J., Ismail, R., Saputra, E., Sugiyanto, S. and Anwar, I.B., (2014) 'The effect of repeated impingement on UHMWPE material in artificial hip joint during salat activities', *Adv. Mat. Res.*, Vol. 896, pp. 272-275.

Kurtz, S.T., Pruitt, L., Jewett, C.W., Crawford, R.P., Crane, D.J. and Edidin, A.A. (1998) 'The yielding, plastic flow, and fracture behavior of ultra-high molecular polyethylene used in total joint replacements', *Biomaterials*, Vol. 19, pp. 1989-2003.

McNie, C., Barton, D.C., Stone, M.H. and Fisher, J. (1998) 'Prediction of plastic strains in ultra-high molecular weight polyethylene due to microscopic asperity interactions during sliding wear', *Proc. Inst. Mech. Eng. H*, No. 212, pp. 49-56.

Saputra, E., Anwar, I.B., Ismail, R., Jamari, J. and van der Heide, E. (2014) 'Numerical simulation of artificial hip joint movement for Western and Japanese-style activities', *J Teknologi (Sci. & Eng.)*, Vol. 66, No. 3, pp. 53-58.

Saputra, E., Anwar, I.B., Jamari, J. and van der Heide, E. (2013) 'Finite element analysis of artificial hip joint movement during human activities', *Procedia Eng.*, No. 68, pp. 102-108.

Scifert, C.F., Brown, T.D., Pedersen, D.R. and Callaghan, J.J. (1998) 'A finite element analysis of factors influencing total hip dislocation', *Clin. Orthop.*, Vol. 355, pp. 152-162.

Sikes, C.V., Lai, L.P., Schreiber, M., Mont, M.A., Jinnah, R.H. and Seyler, T.M. (2008) 'Instability after total hip arthroplasty treatment with large femoral heads vs constrained liners', *J. Arthrop.*, Vol. 23, No.7, pp. 59-63.

Sugano, N., Tsuda, K., Miki, H., Takao, M., Suzuki, N. and Nakamura, N. (2012) 'Dynamic measurements of hip movement in deep bending activities after total hip arthroplasty using a 4-dimensional motion analysis system', *J. Arthrop.*, Vol. 27, No. 8, pp. 1562-1568.

Tanino, H., Harman, M.K., Banks, S.A. and Hodge, W.A. (2007) 'Association between dislocation, impingement, and articular geometry in retrieved acetabular polyethylene cups', *J. Orthop. Res.*, Vol. 25, No. 11, pp. 1401-1407.